HHS Public Access

Author manuscript

Cytotherapy. Author manuscript; available in PMC 2017 February 01.

Published in final edited form as:

Cytotherapy. 2016 February ; 18(2): 263–277. doi:10.1016/j.jcyt.2015.10.015.

Collagen Type II Enhances Chondrogenic Differentiation in Agarose-based Modular Microtissues

Ramkumar Tiruvannamalai Annamalai, **David Mertz**, **Ethan L.H. Daley**, and **Jan P. Stegemann***

Department of Biomedical Engineering, University of Michigan, Ann Arbor, Michigan

Abstract

Background—Cell-based therapies have made an impact on the treatment of osteoarthritis, however the repair and regeneration of thick cartilage defects is an important and growing clinical problem. Next-generation therapies that combine cells with biomaterials may provide improved outcomes. We have developed modular microenvironments that mimic the composition of articular cartilage as a delivery system for consistently differentiated cells.

Methods—Human bone marrow-derived mesenchymal stem cells (MSC) were embedded in modular microbeads consisting of agarose (AG) supplemented with 0%, 10%, and 20% collagen Type II (COL-II) using a water-in-oil emulsion technique. AG and AG/COL-II microbeads were characterized in terms of their structural integrity, size distribution, and protein content. The viability of embedded MSC and their ability to differentiate into osteogenic, adipogenic and chondrogenic lineages over three weeks in culture were also assessed.

Results—Microbeads made with <20% COL-II were robust, generally spheroidal in shape and 80 ± 10 μm in diameter. MSC viability in microbeads was consistently high over a week in culture, while viability in corresponding bulk hydrogels decreased with increasing COL-II content. Osteogenic differentiation of MSC was modestly supported in both AG and AG/COL-II microbeads, while adipogenic differentiation was strongly inhibited in COL-II containing microbeads. Chondrogenic differentiation of MSC was clearly promoted in microbeads containing COL-II, compared to pure AG matrices.

Conclusions—Inclusion of collagen Type II in agarose matrices in microbead format can potentiate chondrogenic differentiation of human MSC. Such compositionally tailored microtissues may find utility for cell delivery in next-generation cartilage repair therapies.

Graphical abstract

*Corresponding Author: Jan P. Stegemann, Department of Biomedical Engineering, University of Michigan, 1101 Beal Ave., Ann Arbor, MI 48109, Tel: 734-764-8313, Fax: 734-647-4834, jpsteg@umich.edu.

Disclosure of Interest: The authors have no conflicts to disclose.

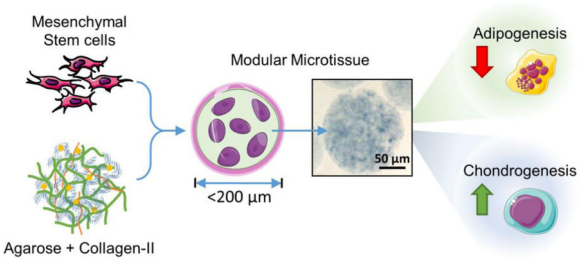

Keywords

microencapsulation; modular tissue engineering; chondrogenesis; agarose; collagen; cartilage tissue engineering; mesenchymal stem cells; biomaterials

Introduction

Repair and regeneration of cartilage is a difficult orthopedic problem due to the low inherent healing capacity of the native tissue [1–3]. Articular cartilage is a well-organized tissue with remarkable durability, however damage may result in debilitating joint pain and functional impairment. Clinical approaches such as osteotomy and osteochondral graft transplantation [4] have shown benefits in terms of relieving pain, delaying further deterioration and restoring partial function, but these therapies do not result in the regeneration of fully competent tissues and their sustainability in a load-bearing environment remains uncertain. The lack of long-term clinical solutions for cartilage repair has motivated the search for improved regenerative therapies that achieve full recovery of intractable and large defects.

Cell-based approaches have emerged as a clinical therapy to regenerate damaged cartilage [5–10]. However, challenges associated with naked chondrocyte delivery [11, 12] have led to the development of matrix-assisted strategies for cell implantation [13–16]. Such biomaterial-based approaches use a preformed scaffold or a hydrogel matrix, often supplemented with biochemical cues, to provide mechanical stability while sustaining chondrogenic differentiation. It has also been shown that native extracellular matrix components in combination with autologous cells can to some degree recapitulate the native microenvironment and architecture, which can improve clinical outcomes [17]. Pre-clinical studies have also shown that cell-seeded scaffolds can be maintained in perfusion cultures with exogenous stimuli before implantation to further improve graft maturation and host-implant integration [18–20]. Despite these efforts, a repair tissue with functional properties and stability comparable to articular cartilage has yet to be engineered.

Bone marrow-derived mesenchymal stem cells (MSC) have been investigated widely for cartilage repair applications [21–24]. These progenitor cells are readily available, have demonstrated multi-lineage potential [25], and also exhibit valuable immunomodulatory and tissue homing properties [26]. MSC have been shown to differentiate into both cartilage [27–30] and bone [31–33], supporting their use in orthopaedic applications. In addition, MSC can exhibit both trophic [34] and chemotactic effects [35] to create a regenerative tissue environment. Notably, even MSC isolated from the marrow of patients with advanced

osteoarthritis retain their chondrogenic potential and synthesize cartilage-specific matrix [27]. Taken together, the tissue-specific and pro-regenerative capabilities of MSC make them an excellent cell source for engineering of cartilage tissue. Combination of MSC with an appropriate biomaterial scaffold that mimics key aspects of the native extracellular matrix architecture and biochemistry may further enhance their regenerative potential.

The major material components of articular cartilage are large proteoglycans with interspersed fibrillar collagen, which constitute about 15–25% and 50–60% of dry weight, respectively [36–39]. Proteoglycans contribute to the compressive stiffness of the cartilage while the tensile strength and resilience are dependent on collagen fibers [40]. In articular cartilage, chondrocytes are embedded in the matrix at a relatively low cell density (~10^4 cells/mm^3) and account for only about 1% of the tissue volume [41, 42]. In their native differentiated state, chondrocytes have a generally spheroidal morphology and synthesize collagen Type II and large proteoglycans. However, when isolated and placed in conventional 2D culture chondrocytes will dedifferentiate, spread on the culture surface, and produce predominantly collagen type I and small proteoglycans [43–45]. While collagen Type I is commonly used as a scaffold in tissue engineering because of its wide availability [46, 47], it has been shown that collagen Type II can preferentially promote cell proliferation, ECM deposition and wound healing by chondrocytes [48–50]. The polysaccharide agarose has been used as a mimic of the proteoglycan component of cartilage, and has been shown to maintain the spherical morphology of chondrocytes [51, 52], as well as support the deposition of an appropriate pericellular matrix [51–54]. In vivo studies have demonstrated that agarose provides a microenvironment that supports the non-hypertrophic and non-proliferative chondrogenic phenotype [55]. The physiological response to agarose resembles a wound-healing response similar to other biomaterials commonly used in the context of tissue repair [56]. Studies in both animals and humans have shown that agarose can be completely biodegraded and cleared after implantation without adverse effects [55, 57].

The goal of the present study was to fabricate and characterize modular microenvironments that mimic the proteoglycan-protein composition of cartilage tissue, with an emphasis on the ability to support lineage-specific differentiation of human bone marrow-derived MSC. The proteoglycan component was represented by agarose (AG), a polysaccharide that can easily be formed into a hydrogel and which has found utility as a matrix in cartilage tissue engineering [51, 58]. The protein component was represented by reconstituted collagen Type II (COL-II), which can form fibrillar structures as in the native tissue [37]. Cells were embedded directly into the AG/COL-II matrix using a water-in-oil emulsion technique, which produced discrete “microbeads” (~80 μm in diameter) consisting of MSC embedded in a spheroidal hydrogel matrix. The modular format has several potential advantages over bulk gel methods in terms of reducing diffusion path lengths, allowing pre-culture of matrix-adhered cells, and delivering a differentiated cell population. Microbeads made with specific COL-II contents were characterized for their structural integrity, size distribution, and protein content. MSC viability and their potential to differentiate into osteogenic, adipogenic, and chondrogenic lineages were also assessed. The long-term goal of this work is to develop injectable, cell-based, modular microenvironments that promote specific tissue regeneration, as shown schematically in Figure 1 in the case of articular cartilage. Such a

therapy would provide a 3D matrix environment and cells of specified function that could be delivered minimally invasively to sites of tissue damage.

Materials and Methods

Biopolymers and MSC culture

Agarose (AG, Fisher Scientific, Hampton, NH) was low melting point grade with an average molecular weight of 120 kDa, gelling temperature between 34.5–37.5 °C and gel-strength of ~500 g/cm^{2}min. AG stock solution was made at 2.0 wt% by dissolving the appropriate amount of powdered AG in DI water heated to 60 °C, and sterilized using a 0.2 μm filter. Collagen Type II (COL-II, Elastin Products Company, Owensville, MO) was from mouse sternum with a molecular weight of 1000 kDa, less than 0.4% proteoglycan, and was tested for the absence for collagen Type-I. COL-II stock solution was made at a concentration of 0.4 wt% by dissolving sterile lyophilized COL-II in 0.02 N acetic acid solution.

Human bone marrow derived mesenchymal stem cells (MSC) were obtained from a commercial vendor (RoosterBio Inc., Frederick MD). The cells were from an individual male donor 31–45 years of age. These cells tested positive for CD166, CD105, CD90, and CD73, and negative for CD14, CD34 and CD45. Cells were expanded in standard MSC growth medium consisting of α-MEM (Gibco Life Technologies, Carlsbad, CA) supplemented with 10% MSC-FBS (Gibco) and penicillin (50 U/mL)/streptomycin sulfate (50 μg/100mL, Gibco). MSC from passage 4–7 were maintained at 37.0 °C in standard cell culture incubators and the medium was replenished every two days. For encapsulated cultures, the microbeads were suspended in a suitable volume of cell culture medium and maintained in 15 mL vented polypropylene bio-reaction tubes (Celltreat, Shirley, MA).

Microbead and bulk gel fabrication and characterization

Cells were encapsulated in AG and AG/COL-II microbeads at a concentration of 0.5 million cells/mL using an adaptation of a water-in-oil emulsification procedure described previously [46], and the final concentrations of each component in the microbead formulations are listed in Table 1. Briefly, MSC were suspended in matrix solution consisting of AG and COL-II solutions, 0.1 N Sodium Hydroxide (Sigma, St. Louis, MO) and 10% FBS (Gibco). The cell-matrix mixture was injected into 80 mL of stirred polydimethylsiloxane (PDMS, PMX-200, 100 cS; Xiameter Dow Corning, Midland, MI). Emulsification was carried out using an impeller speed of 800 rpm. Immediately following injection of the cell-matrix suspension, the PDMS was kept at 37°C for 5 min using a water bath. Once the matrix suspension was emulsified, the water bath was replaced with a crushed ice bath and stirred for a further 25 min. The resulting microbeads were then separated from the oil phase by centrifugation at 150 g for 5 min. Microbeads were washed twice in MSC culture medium and maintained under standard culture conditions. The microbead format allowed aliquoting of precise volumes of suspended microbeads for use in biochemical and other assays. For microbead maintenance, the culture medium was replenished every second day. Bulk hydrogel constructs were also made for comparison to microbeads at the same cell concentration. For bulk gels, MSC were suspended in the corresponding hydrogel solution and after through mixing the hydrogel was poured into glass bottom petri dishes and allowed

to gel at 37 °C for 30 min. Gelled bulk constructs were approximately 1.5 mm in thickness. Culture medium was added on top of each gel and cultures were maintained at 37 °C.

Freshly made microbeads were imaged using an inverted phase-contrast microscope (Nikon). Four random fields were imaged for each formulation, totaling approximately 150 microbeads in each count. Microbead diameter was measured manually using Image J software (National Institutes of Health) to determine the size distribution of the formulations tested. Microbeads were also visualized microscopically to determine their structural integrity. The formulations were qualitatively assessed based on the ratio of intact microbeads to broken or fragmented microbeads in a specific volume of the sample.

Collagen content in the microbeads was analyzed via protein staining using Coomasie Blue G-250 (Bio-Rad). Staining solution was made by adding 10 mL glacial acetic acid to 45 mL double-distilled water. 300 mg of powdered Coomasie Blue was then dissolved in 45 mL of methanol and the two solutions were combined and sterile-filtered. The microbeads were suspended in the staining solution for 5 min and washed multiple times in PBS to remove nonspecific binding. The microbeads were then observed imaged with a bright field microscope (Nikon).

Analysis of MSC morphology and viability

Cells were encapsulated in microbeads and cultured for one week to study short-term viability and cell morphology. For live/dead assay, Calcein-AM (4.0 mM), ethidium homodimer (2.0 mM) and DAPI (2.0 μg/mL) solutions were used (Molecular Probes). After aspirating the culture medium, microbeads were washed in PBS and incubated in dye solution at 37°C for 45 min. After two washes in 10 mM PBS, microbeads were re-suspended in fresh PBS and imaged under an inverted fluorescence microscope (Nikon) using filter sets for green and red (Excitation/Emission 488/530 for calcein-AM and 488/630 for ethidium homodimer). Multiple non-overlapping images were taken for every sample and the percentage of viable cells was quantified using Image J. Briefly, 16 bit TIF images were separated into 8 bit red and green channels and converted to binary images for particle analysis counts. For cell morphology analysis, Texas Red®-phalloidin (Molecular Probes, Life Technologies, Grand Island, NY) was used to stain cytoskeletal actin with DAPI as a nuclei counterstain. Samples were washed twice with PBS and fixed with Z-fix fixative for 10 min at 4 °C. After permeabilization with 0.5% Triton X-100 in PBS for 20 minutes at room temperature, the samples were washed twice in PBS and stained with Texas Red®-phalloidin (1:40 dilution) and DAPI (2 ng/mL) for 45 min at room temperature. Finally, after two more PBS washes, the samples were imaged using a fluorescence microscope (Nikon).

Quantitation of protein and DNA content

A commercially available double stranded-DNA assay kit was used (Quanti-iT™ PicoGreen, Invitrogen, Life Technologies, Grand Island, NY) to quantify DNA content, which is reflective of cell content. Microbead samples were washed in PBS and digested in 50 mM Tris-HCl/4 M Guanidine-HCl solution (pH-7.5) for 2–3 hours at 4°C. Digested samples were then centrifuged at 500×g and the samples were diluted 5 times in DI water to

reduce the guanidine concentration to below 150 mM to avoid interference. The DNA content in the supernatant was then quantified using 1X PicoGreen in Tris-HCl buffer added to the diluted samples by measuring fluorescence at EX:485, EM:518 nm after 5 min incubation. Purified calf thymus DNA served as the standard for the assay.

The COL-II content of the fabricated microbeads was verified using a commercially available total protein assay kit (BCA Protein Assay Reagent Kit, Pierce, Rockford, IL). Microbead samples were washed three times in PBS and suspended in ice-cold PBS, and then sonicated (Branson Ultrasonics, Danbury, CT) for 20 s, with a 10 s interval to avoid heat denaturation. Homogenized samples were then diluted three times in DI water and the protein content was quantified according to the manufacturer's protocol. Purified bovine serum albumin (BSA) served as the standard for the assay.

Histology

Microbeads were fixed overnight in buffered zinc formalin (Z-Fix, Anatech Ltd, Battle Creek, MI), embedded in 12 mm diameter collagen gel (3.0 mg/ml) disks and fixed again for 2 h. Disks were then infiltrated with paraffin using an automated tissue processor (TP1020, Leica Biosystems, Buffalo Grove, IL), embedded in paraffin blocks and cut into 6 μm sections using a rotary microtome. To differentiate the acidic mucins indicative of chondrogenesis from neutral mucins, Alcian Blue (AB)-Periodic Acid Schiff's (PAS) staining was carried out using a commercially available kit (Polyscientific R&D Corp, Bayshore, NY) according to the manufacturer's protocol. The sections were then imaged with a brightfield microscope (Nikon).

Osteogenic, adipogenic and chondrogenic differentiation

Osteogenic differentiation medium consisted of growth medium (α-MEM, 10% FBS) supplemented with 0.2 mM l-ascorbic acid 2-phosphate (Sigma), 10 mM β-glycerophosphate (Sigma), and 100 nM dexamethasone (Sigma). Osteogenic differentiation of MSC was assessed by quantifying osteocalcin secretion and calcium deposition of functional osteoblasts. Osteocalcin is a protein secreted by mature osteoblasts, and is a marker for osteogenesis [59]. Microbeads were washed in PBS and digested in 0.2 N HCl overnight at 37 °C and neutralized before the assay using 10 N NaOH. A human intact-osteocalcin ELISA kit (Alpha Aesar, Ward Hill, MA) was used to quantify intact osteocalcin present in the samples. This ELISA kit is specific for intact osteocalcin (1–49 amino acid residues) and not for fragments of the protein, and was used according to the manufacturer's protocol. In brief, samples were added to a pre-coated (captured monoclonal antibody) 96 well plate. HRP-Conjugated Streptavidin was then added and developed (Strep-Av-HRP), and absorbance was measured at 450 nm. Purified human osteocalcin served as standards. For analysis of calcium deposition, microbead samples were fixed in 10% buffered zinc-formalin (Anatech, Battle Creek, MI) and washed three times in PBS and twice in DI water before the assay. The samples were then stained in 1.0% Alizarin Red solution for 10 min prepared by dissolving 1.0 g of Alizarin Red powder (Sigma) in 100 mL of ultrapure water (pH 4.2). The microbeads were then washed in DI water twice and detained in 1.0 mL of 0.5 N HCl/5% SDS solution for 20 min. The destained extracted solution was then sampled and quantified calorimetrically by measuring absorbance at 415 nm.

Adipogenic medium consisted of α-MEM supplemented with 10% FBS, 10 μg/mL human recombinant insulin (Sigma), 0.5 mM 3-isobutyl-1-methylxanthine (IBMX) and 1 μM dexamethasone. Adipogenic differentiation of MSC was assessed by quantifying the total lipid content of the cells. Microbead samples were fixed in 10% buffered zinc-formalin (Anatech) and washed three times in PBS and once in 60% propylene glycol before the assay. The samples were then stained with warm Oil Red O staining solution (0.5% in propylene glycol, Sigma) for 10 min. The samples were then washed in 85% propylene glycol solution for 2 min, followed by DI water for 2 min. The stained samples were destained using 100% isopropanol for 15 min, and the extracted solution was sampled and quantified calorimetrically by measuring absorbance at 500 nm.

The chondrogenic differentiation medium consisted of DMEM-high glucose supplemented with 1% FBS, 1% ITS Premix Universal Culture Supplement (Corning), 0.35 mM l-proline (Sigma), 1 mM sodium pyruvate (Gibco), l-glutamine (4mM, Gibco), 0.2 mM l-ascorbic acid 2-phosphate (Sigma), 100 nM dexamethasone (Sigma) and 10 ng/mL rhTGF-b1 (Peprotech, Rocky Hill, NJ). Chondrogenic differentiation of MSC was assessed by quantifying sulfated glycosaminoglycans (sGAG) deposited by functional chondrocytes. Microbeads were washed in PBS and digested using papain extraction solution consisting of 20 μg/mL crystallized papain suspension (Corning), 0.2 M sodium phosphate (Sigma), 0.1 M sodium acetate (Sigma), 0.01 M EDTA (Sigma), and 5 mM L-cysteine (Sigma). sGAG in the papain-digested microbeads was quantified using 1,9-dimethylmethylene blue (DMMB) as previously reported [60, 61]. Briefly, 25 μL of the sample was added to 200 μL of DMMB and the absorbance of the solution was measured at 525 nm. Purified chondroitin sulfate (Sigma) from shark cartilage was used for standards. All conditions were sampled and analyzed in triplicate.

Statistical analysis

All measurements were performed at least in triplicate. Data are plotted as means with error bars representing standard deviation. Statistical comparisons were done using Student's t-test with a 95% confidence limit. Differences with $p<0.05$ were considered statistically significant.

Results

Microbead fabrication and characterization

Microbeads made at AG/COL-II mass ratios shown in Table 1 were characterized one day after fabrication in terms of general morphology, population size distribution, structural integrity and collagen content. Phase-contrast and brightfield images of representative microbeads are shown in Figure 2A. Pure AG microbeads were essentially transparent and smooth, compared to the visibly more textured appearance that was evident with increasing collagen content. A similar trend was seen when microbeads were stained for protein using Coomasie Blue (Fig. 2B), with the degree of texture and staining increasing with COL-II content. The median microbead diameter (Fig. 2C) was approximately 80 ± 10 μm, regardless of composition, however the variation in microbead size increased marginally with increasing COL-II content. Microbeads made with 20 wt% COL-II were fragile but

could be processed, whereas at COL-II concentrations greater than 20 wt% the microbeads exhibited insufficient integrity for further study (data not shown). Quantitative of the protein content of microbeads (Fig. 2D) showed a linear increase in collagen concentration with increasing mass of collagen used for microbead fabrication ($R^2 = 0.97$).

MSC morphology and viability in AG/COL-II matrices

The morphology of MSC embedded in matrix formulations containing 0%, 10%, and 20% COL-II was assessed by staining the actin cytoskeleton of MSC entrapped in bulk gels (Fig. 3A) and microbeads (Fig. 3B). In pure AG bulk gels, MSC were highly rounded with very little spreading, while the degree of spreading and pseudopod extension increased in the 10% and 20% COL-II bulk gels. A very similar trend was observed in the AG/COL-II microbead format, in which cells in COL-II-containing matrices showing increased spreading and extension of pseudopods, which was particularly evident in the microbeads containing 20% COL-II.

Quantitation of the DNA content of microbeads (Fig. 3C) showed that those fabricated with pure AG and 10% COL-II contained the same number of cells at fabrication. The viability of MSC embedded bulk gels and microbeads assayed one day after fabrication is shown in Figure 3D. Cells showed generally high viability across all matrix formulations. In bulk gels, MSC viability was above 85% in the 0% and 10% COL-II formulations, though bulk gels containing 20% COL-II exhibited a lower initial viability around 70%. In microbeads, MSC viability was consistently above 75% in all formulations. Microbeads were precultured in expansion medium for a period of 1 week prior to being exposed to differentiation media, and viability remained high during this preculture period.

Osteogenic differentiation of MSC in microbeads

Lineage-specific differentiation of MSC encapsulated in AG and AG/COL-II microbeads was assessed over time in culture. Because of the relative fragility of microbeads with 20% COL-II content, the multilineage differentiation experiments were performed using only pure AG (control) microbeads and the 10% COL-II microbead formulation, at an MSC concentration of 0.5×10^6 cells/mL hydrogel. Microbeads were initially maintained in MSC expansion medium for a 1-week preculture period to allow acclimation post-encapsulation, and were subsequently switched to lineage-specific medium and cultured for a further 21 days to induce differentiation. In the description of results below, the day of analysis refers to the number of days of differentiation culture, such that “Day 7” refers to the time point at which the microbeads have been in lineage-specific medium for 7 days.

Results from osteogenic differentiation experiments are shown in Figure 4. The images in panel 4A show DIC images of microbeads and confocal fluorescence images of cell viability using a vital stain over time in culture. Microbeads maintained their integrity throughout the culture period. MSC morphology was generally spherical, though evidence of moderate cell spreading can be seen in the AG/COL-II microbeads, particularly at the later time point. MSC viability is shown in Table 2, and was higher in AG/COL-II microbeads (75–85%), compared to pure AG microbeads (60–70%) at both early and later time points. The DNA content in differentiating microbead populations (Fig. 4B) was used to estimate cell content.

In pure AG microbeads, DNA content was essentially constant over the differentiation culture period, though tended towards a decrease at later time points. In AG/COL-II microbeads, the cell content started at a lower level than pure AG samples, but exhibited a steady increase over time in culture, such that at day 21 the total DNA content in 10% COL-II microbeads was significantly higher than that of pure AG microbeads ($p<0.05$).

Osteocalcin production (Fig. 4C) increased in both pure AG and AG/COL-II microbeads by 21 days in osteogenic culture, and was significantly higher in the populations cultured in osteogenic medium ($p<0.05$) compared to the control medium. However, there was no statistically significant difference between AG and AG/COL-II microbeads maintained under osteogenic conditions at any time point. In addition, when cultured in control medium, there was a significant decrease in osteocalcin production in AG/COL-II beads compared to AG beads. Calcium deposition was assessed using an Alizarin Red assay (Fig. 4D), and followed a similar trend, showing a significant increase from day 1 to day 21 in both pure AG and AG/COL-II microbeads, but no significant between the two matrices. The calcium deposition data were reinforced by the DIC images of microbeads, which showed an accumulation of material and a more opaque appearance in microbeads cultured in osteogenic medium over time, presumably due to the deposition of calcium phosphate mineral by differentiating MSC.

Adipogenic differentiation of MSC in microbeads

MSC encapsulated in pure AG and AG/COL-II were also subjected to an adipogenic differentiation protocol consisting of acclimation culture in control MSC expansion medium for 7 days followed by 21 days of culture in adipogenic medium. DIC images of microbeads and confocal fluorescence images of vital-stained embedded cells (Fig. 5A) show that the microbeads retained their integrity over time in adipogenic culture. MSC viability in AG/COL-II microbeads was somewhat lower (~60%, Table 2) at day 7, compared to pure AG microbeads (~80%), but by day 21 both formulations exhibited similarly high cell viability (80–85%).

Measurement of DNA (Fig. 5B) showed that in pure AG microbeads there was a significant drop in cell content from day 7 to day 21 in pure AG microbeads ($p<0.05$), while AG/COL-II microbeads exhibited a steady and statistically significant increase in cell content from day 7 to day 21 ($p<0.05$). A quantitative colorimetric assay using Oil Red-O (Fig. 5C) showed a 6-fold increase ($p<0.001$) in intracellular lipid droplet accumulation in pure AG microbeads maintained in adipogenic medium, compared to that of pure AG microbeads cultured in control medium, and a 3-fold increase ($p<0.001$) compared to AG/COL-II microbeads maintained in adipogenic medium. However, AG/COL-II microbeads cultured in adipogenic differentiation medium did not show a significant increase in lipid content, relative to control medium cultures. The DIC and fluorescence images show an increased cell volume in adipogenic cultures, which can be attributed to lipid accumulation and was more pronounced in pure AG microbeads compared to AG/COL-II microbeads.

Chondrogenic differentiation of MSC in microbeads

Pure AG and AG/COL-II microbeads were also cultured in chondrogenic differentiation medium for 21 days, after an initial 7 day acclimation period in control MSC medium. DIC images (Fig. 6A) showed that microbeads retained their generally spherical shape and integrity throughout the culture period. Corresponding confocal fluorescence images showed cell shape, which remained generally rounded and exhibited clustering by day 21. MSC viability, shown by vital staining in Fig. 6A and presented quantitatively in Table 2, was initially very high in AG microbeads in expansion medium and somewhat lower in lineage-specific media. In chondrogenic medium, viability in pure AG microbeads dropped from ~60% to ~30% over the 21-day differentiation culture period. In contrast, viability in AG/COL-II microbeads remained essentially constant at ~60–70% over time in culture.

Pure AG microbeads showed a steady decline in DNA content (Fig. 6B) over time in chondrogenic culture, and cell content at day 21 was significantly lower than at day 0 ($p<0.05$). In AG/COL-II microbeads, the initial cell content was lower but stayed more constant over time in culture, and was statistically unchanged over 21 days. Deposition of sGAG, a marker of chondrogenic phenotype (Fig. 6C), generally increased over time in culture in both AG and AG/COL-II microbeads. Chondrogenic differentiation was particularly evident in AG/COL-II microbeads, which had statistically significantly higher sGAG deposition by day 14 ($p<0.05$), and by day 21 showed a 60% increase over their pure AG counterparts. Staining of histological sections with Alcian Blue (AB)-Periodic Acid Schiff (PAS) to detect polysaccharides (Fig. 7) confirmed a rounded morphology and relatively little matrix deposition in pure AG microbeads cultured in chondrogenic medium (Fig. 7A, 7B). In contrast, AG/COL-II microbeads cultured in chondrogenic conditions (Fig. 7C, 7D) exhibited clearly more robust polysaccharide matrix deposition at both day 7 and 21. The overlaid DIC and calcein-AM fluorescence images in Figure 7 also show that the differentiating MSC maintained a rounded morphology, with visible matrix deposition around the cells.

Discussion

Creation of cellular microenvironments that mimic cartilage tissue has been approached in a variety of ways [4, 5, 8, 13, 24]. In the present study, our goal was to fabricate and characterize modular microtissues that mimic both the proteoglycan content and the protein content of native cartilage. To this end, we created microbeads consisting of various mass ratios of the polysaccharide agarose and the protein collagen Type II. Agarose has been used previously as a matrix in cartilage tissue engineering. While this polysaccharide does not recapitulate all of the properties of cartilage proteoglycans, it has been shown to have relevance in directing cell phenotype [53–55, 58]. The protein collagen Type II is highly associated with hyaline cartilage, but has not been used widely as a scaffold material because of its relative scarcity. By creating microscale polysaccharide-protein tissue constructs, we aimed to harness the mechanical robustness of agarose gels, while also augmenting the matrix with a tissue-specific protein isoform.

MSC were chosen as a cell source because of their demonstrated ability to differentiate into specific tissue lineages, including orthopaedic tissues, under the appropriate stimulation

[27–33]. A major advantage of using MSC as a cell source in cartilage tissue engineering is that they can be expanded to clinically significant numbers without loss of their undifferentiated phenotype [62]. In the present study we used a commercially available source of MSC, and future work will need to address variability between cells from different donors, and their capacity for differentiation. Well-characterized and expanded cell populations can then be differentiated toward the chondrocytic phenotype for use in cell-based therapies for cartilage repair. In contrast, removal of chondrocytes from their native environment and expansion in monolayers can cause dedifferentiation and loss of function [43–45]. Partial function may be recovered by transferring cultured chondrocytes to a 3D environment, but the recovery is incomplete [51, 52]. Donor site morbidity also limits the use of autologous chondrocytes, as any defect to healthy cartilage may further degenerate the surrounding tissue [63]. A consistent progenitor cell source and methods for reliably differentiating and delivering such cells is therefore an important need for cell-based therapies.

The system we used to fabricate polysaccharide-protein microbeads is an adaptation of a method that we have used for a variety of modular tissue engineering applications [64–68]. This water-in-oil emulsion process is easy to implement and creates large batches of essentially identical microbeads in a short period of time. The average size and size distribution of the microbeads can be tailored by controlling the impeller geometry, the impeller-to-vessel diameter ratio, and the viscosity of the dispersed phases [69, 70], and the process can be scaled to create smaller (<1 mL) or larger (>10 mL) volumes of microbeads. Emulsification produces microbead populations with a distribution of sizes, which can be an advantage when creating packed beds of microbeads, but it is difficult to tightly control microbead size. The composition of the microbeads is determined by controlling the type and amount of constituents that make up the aqueous phase, including the cell type. A variety of gelable materials and relevant cell types have been used in this system, and they are being investigated for advanced biomaterial-based cell delivery. More broadly, modular approaches to creating engineered tissue are emerging as a promising approach to creating complex structures [71–76]. Such methods have advantages over conventional scaffold-based techniques [64, 72], and new methods are being developed at a rapid rate.

In the present study, we created hydrogel microbeads by mixing AG and COL-II in specific mass ratios. MSC were embedded directly in the microbead matrix at the time of gelation by suspending them in the matrix formulation used to create the microbeads. All the AG/COL-II hydrogel formulations we tested emulsified consistently, however retrieval of the formed microbeads from the oil phase became challenging as the COL-II mass concentration was increased. Microbeads made with ≥20% COL-II were fragile and broke apart during collection, and therefore were not suitable for long term cultures. In contrast, microbeads fabricated with <20% COL-II were more robust and stayed intact over time in culture. The relatively strong gel formed by the AG component aided in protecting microbeads from compressive forces during the emulsification and collection processes, since in a polysaccharide-protein co-gel such as AG/COL-II the non-fibrillar component significantly enhances the mechanical properties in compression [77, 78]. The median microbead diameter in the present work was 80 ± 10 μm in all formulations, but the consistency of microbead size also decreased with an increase in COL-II content, presumably due to the

increase in viscosity caused by the addition of a macromolecular protein component. The decrease in microbead integrity and increase in size heterogeneity in formulations ≥20% COL-II led us to focus on microbeads with 10% COL-II in this study, which were compared to pure AG controls.

MSC were shown to remain viable upon encapsulation in AG/COL-II microbeads, with only minor loss of cell viability 24 hours after encapsulation, and maintenance of high cell viability over 7 days when cultured in standard MSC expansion medium. By day 7, cell viability in all hydrogel formulations was also significantly higher in 3D microbeads compared to bulk gels made at the same matrix composition. This effect may be attributed to the increased access to oxygen and other nutrients that microbeads can provide due to their small size and associated short diffusion distances [79]. Increasing the COL-II concentration in microbeads resulted in a noticeable increase in cell spreading within the matrix, presumably as a consequence of integrin-mediated cell attachment to the protein component. While COL-II has been associated with increased chondrogenic differentiation of MSC [80, 81], it has also been suggested that a nonspherical morphology can result in dedifferentiation of chondrocytes [62]. Therefore it is important to balance the effects of added extracellular matrix components in microbead formulations.

Our main interest in this study was the ability of microbeads to support desired tissue-specific differentiation. We therefore compared the multilineage potential of MSC embedded in AG/COL-II (10%) microbeads and pure AG microbeads over three weeks of culture. Osteogenic differentiation was modestly supported by both pure AG and AG/COL-II formulations, as evidenced by an increase in osteocalcin expression and calcium deposition after 21 days in osteogenic medium. However, there was no difference between the matrix formulations in their ability to promote osteogenesis *in vitro*. Pure AG microbeads cultured in adipogenic medium showed robust lipid accumulation after 21 days, while AG/COL-II microbeads produced only low levels of lipid even when exposed to adipogenic stimuli. In contrast, chondrogenesis was significantly more robust in AG/COL-II microbeads, compared to pure AG, and strong expression of sGAG was measured by days 14 and 21 in chondrogenic culture. Deposition of sGAG was confirmed using histology, which showed rounded cells and more matrix deposition in the COL-II-containing microbeads. These data suggest that the inclusion of COL-II in agarose microbeads can potentiate differentiation toward the chondrogenic lineage, while inhibiting adipogenic differentiation. The mechanism of this effect is not clear from our experiments, however binding of MSC to specific proteins has been shown to modulate differentiation [82, 83]. In addition, it has been suggested that cryptic peptide sequences on the COL-II molecule can affect chondrocyte phenotype [1].

In summary, we have demonstrated a method for creating modular microtissues designed to mimic specific proteoglycan and protein components of the cartilage extracellular matrix. The resulting MSC-laden microbeads are robust, support cell viability, and can be maintained in culture. Further, our data show that the composition of the 3D matrix in the microbeads affects the lineage-specific differentiation of embedded MSC. In particular, COL-II was shown to preferentially promote the chondrogenic phenotype, while suppressing adipogenic differentiation. The microbead format has the advantage that diffusion path

lengths are short, and microbead preparations can be delivered in a minimally invasive manner. The composition of microbeads can also be varied to include other cell and matrix types, and to incorporate biochemical factors that promote the desired regenerative effects. Cartilage defects are a serious and growing problem, and cell-based therapies have started to have an impact on their treatment. The development of biomaterial-based approaches that improve cell differentiation, delivery, and function will enable the next generation of cell-based cartilage therapies.

Acknowledgments

Research reported in this publication was supported in part by the National Institute of Arthritis and Musculoskeletal and Skin Diseases of the National Institutes of Health under award numbers R21AR062709 and R01AR062636. The content is solely the responsibility of the authors and does not necessarily represent the official views of the National Institutes of Health.

References

1. Hunziker EB. Articular cartilage repair: basic science and clinical progress. A review of the current status and prospects. Osteoarthritis and Cartilage. 2002; 10(6):432–463. [PubMed: 12056848]
2. Hunziker EB, et al. An educational review of cartilage repair: precepts & practice – myths & misconceptions – progress & prospects. Osteoarthritis and Cartilage. 2015; 23(3):334–350. [PubMed: 25534362]
3. Huey DJ, Hu JC, Athanasiou KA. Unlike Bone, Cartilage Regeneration Remains Elusive. Science. 2012; 338(6109):917–921. [PubMed: 23161992]
4. Moran CJ, et al. Restoration of articular cartilage. J Bone Joint Surg Am. 2014; 96(4):336–344. [PubMed: 24553893]
5. Mobasheri A, et al. Chondrocyte and mesenchymal stem cell-based therapies for cartilage repair in osteoarthritis and related orthopaedic conditions. Maturitas. 2014; 78(3):188–198. [PubMed: 24855933]
6. Diekman BO, Guilak F. Stem cell-based therapies for osteoarthritis: Challenges and opportunities. Current opinion in rheumatology. 2013; 25(1):119–126. [PubMed: 23190869]
7. Westreich R, et al. Validating the Subcutaneous Model of Injectable Autologous Cartilage Using a Fibrin Glue Scaffold. The Laryngoscope. 2004; 114(12):2154–2160. [PubMed: 15564836]
8. Crawford DC, et al. An autologous cartilage tissue implant NeoCart for treatment of grade III chondral injury to the distal femur: prospective clinical safety trial at 2 years. Am J Sports Med. 2009; 37(7):1334–1343. [PubMed: 19448048]
9. Medved F, et al. Severe posttraumatic radiocarpal cartilage damage: first report of autologous chondrocyte implantation. Arch Orthop Trauma Surg. 2013; 133(10):1469–1475. [PubMed: 23880842]
10. Crawford DC, DeBerardino TM, Williams RJ 3rd. NeoCart, an autologous cartilage tissue implant, compared with microfracture for treatment of distal femoral cartilage lesions: an FDA phase-II prospective, randomized clinical trial after two years. J Bone Joint Surg Am. 2012; 94(11):979–989. [PubMed: 22637204]
11. Peterson L, et al. Two- to 9-year outcome after autologous chondrocyte transplantation of the knee. Clin Orthop Relat Res. 2000; (374):212–234. [PubMed: 10818982]
12. Niemeyer P, et al. Characteristic complications after autologous chondrocyte implantation for cartilage defects of the knee joint. Am J Sports Med. 2008; 36(11):2091–2099. [PubMed: 18801942]
13. Makris EA, et al. Repair and tissue engineering techniques for articular cartilage. Nat Rev Rheumatol. 2015; 11(1):21–34. [PubMed: 25247412]
14. Musumeci G, et al. New perspectives for articular cartilage repair treatment through tissue engineering: A contemporary review. World J Orthop. 2014; 5(2):80–88. [PubMed: 24829869]

15. Tuan RS. A second-generation autologous chondrocyte implantation approach to the treatment of focal articular cartilage defects. Arthritis Research & Therapy. 2007; 9(5):109–109. [PubMed: 18021426]
16. Harris JD, et al. Failures, re-operations, and complications after autologous chondrocyte implantation – a systematic review. Osteoarthritis and Cartilage. 2011; 19(7):779–791. [PubMed: 21333744]
17. Bornes TD, Adesida AB, Jomha NM. Mesenchymal stem cells in the treatment of traumatic articular cartilage defects: a comprehensive review. Arthritis Res Ther. 2014; 16(5):432. [PubMed: 25606595]
18. Radisic M, et al. Cardiac tissue engineering using perfusion bioreactor systems. Nat Protoc. 2008; 3(4):719–738. [PubMed: 18388955]
19. Chen M, et al. Ectopic osteogenesis of macroscopic tissue constructs assembled from human mesenchymal stem cell-laden microcarriers through in vitro perfusion culture. PLoS One. 2014; 9(10):e109214. [PubMed: 25275528]
20. Pu F, et al. The use of flow perfusion culture and subcutaneous implantation with fibroblast-seeded PLLA-collagen 3D scaffolds for abdominal wall repair. Biomaterials. 2010; 31(15):4330–4340. [PubMed: 20219244]
21. Wang Y, et al. Mesenchymal stem cells for treating articular cartilage defects and osteoarthritis. Cell Transplant. 2014
22. Bian L, et al. Coculture of human mesenchymal stem cells and articular chondrocytes reduces hypertrophy and enhances functional properties of engineered cartilage. Tissue Eng Part A. 2011; 17(7–8):1137–1145. [PubMed: 21142648]
23. Toh WS, et al. Advances in mesenchymal stem cell-based strategies for cartilage repair and regeneration. Stem Cell Rev. 2014; 10(5):686–696. [PubMed: 24869958]
24. Gopal K, Amirhamed HA, Kamarul T. Advances of human bone marrow-derived mesenchymal stem cells in the treatment of cartilage defects: a systematic review. Exp Biol Med (Maywood). 2014; 239(6):663–669. [PubMed: 24764239]
25. Pittenger MF, et al. Multilineage Potential of Adult Human Mesenchymal Stem Cells. Science. 1999; 284(5411):143–147. [PubMed: 10102814]
26. Chamberlain G, et al. Concise Review: Mesenchymal Stem Cells: Their Phenotype, Differentiation Capacity, Immunological Features, and Potential for Homing. STEM CELLS. 2007; 25(11):2739–2749. [PubMed: 17656645]
27. Kafienah W, et al. Three-dimensional cartilage tissue engineering using adult stem cells from osteoarthritis patients. Arthritis & Rheumatism. 2007; 56(1):177–187. [PubMed: 17195220]
28. Ko J-Y, et al. In vitro chondrogenesis and in vivo repair of osteochondral defect with human induced pluripotent stem cells. Biomaterials. 2014; 35(11):3571–3581. [PubMed: 24462354]
29. Wakitani S, et al. Human autologous culture expanded bone marrow mesenchymal cell transplantation for repair of cartilage defects in osteoarthritic knees. Osteoarthritis and Cartilage. 2002; 10(3):199–206. [PubMed: 11869080]
30. Kuroda R, et al. Treatment of a full-thickness articular cartilage defect in the femoral condyle of an athlete with autologous bone-marrow stromal cells. Osteoarthritis and Cartilage. 2007; 15(2):226–231. [PubMed: 17002893]
31. Grayson WL, et al. Stromal cells and stem cells in clinical bone regeneration. Nat Rev Endocrinol. 2015; 11(3):140–150. [PubMed: 25560703]
32. Dupont KM, et al. Human stem cell delivery for treatment of large segmental bone defects. Proceedings of the National Academy of Sciences. 2010; 107(8):3305–3310.
33. Kon E, et al. Autologous bone marrow stromal cells loaded onto porous hydroxyapatite ceramic accelerate bone repair in critical-size defects of sheep long bones. Journal of Biomedical Materials Research. 2000; 49(3):328–337. [PubMed: 10602065]
34. Wu L, et al. Trophic Effects of Mesenchymal Stem Cells in Chondrocyte Co-Cultures are Independent of Culture Conditions and Cell Sources. Tissue Engineering Part A. 2012; 18(15–16):1542–1551. [PubMed: 22429306]
35. Caplan AI. Adult mesenchymal stem cells for tissue engineering versus regenerative medicine. Journal of Cellular Physiology. 2007; 213(2):341–347. [PubMed: 17620285]

36. Poole AR, et al. Composition and structure of articular cartilage: a template for tissue repair. Clin Orthop Relat Res. 2001; (391 Suppl):S26–S33. [PubMed: 11603710]
37. Buckwalter JA, Mankin HJ. Articular cartilage: tissue design and chondrocyte-matrix interactions. Instr Course Lect. 1998; 47:477–486. [PubMed: 9571449]
38. Buckwalter JA, Mankin HJ. Instructional Course Lectures, The American Academy of Orthopaedic Surgeons - Articular Cartilage. Part I. Tissue Design and Chondrocyte-Matrix Interactions*†. 1997; 79:600–611.
39. Sophia Fox AJ, Bedi A, Rodeo SA. The basic science of articular cartilage: structure, composition, and function. Sports Health. 2009; 1(6):461–468. [PubMed: 23015907]
40. Kempson GE, et al. Correlations between stiffness and the chemical constituents of cartilage on the human femoral head. Biochimica et Biophysica Acta (BBA) - General Subjects. 1970; 215(1):70–77. [PubMed: 4250263]
41. Stockwell RA. The cell density of human articular and costal cartilage. Journal of Anatomy. 1967; 101(Pt 4):753–763. [PubMed: 6059823]
42. Hunziker EB, Quinn TM, Häuselmann HJ. Quantitative structural organization of normal adult human articular cartilage. Osteoarthritis and Cartilage. 2002; 10(7):564–572. [PubMed: 12127837]
43. Benya PD, Padilla SR, Nimni ME. Independent regulation of collagen types by chondrocytes during the loss of differentiated function in culture. Cell. 15(4):1313–1321. [PubMed: 729001]
44. Von Der Mark K, et al. Relationship between cell shape and type of collagen synthesised as chondrocytes lose their cartilage phenotype in culture. Nature. 1977; 267(5611):531–532. [PubMed: 559947]
45. Mayne R, et al. Changes in type of collagen synthesized as clones of chick chondrocytes grow and eventually lose division capacity. Proceedings of the National Academy of Sciences of the United States of America. 1976; 73(5):1674–1678. [PubMed: 1064040]
46. Batorsky A, et al. Encapsulation of adult human mesenchymal stem cells within collagen-agarose microenvironments. Biotechnology and Bioengineering. 2005; 92(4):492–500. [PubMed: 16080186]
47. Hunziker EB. Articular cartilage repair: are the intrinsic biological constraints undermining this process insuperable? Osteoarthritis Cartilage. 1999; 7(1):15–28. [PubMed: 10367012]
48. Nehrer S, et al. Canine chondrocytes seeded in type I and type II collagen implants investigated in vitro. J Biomed Mater Res. 1997; 38(2):95–104. [PubMed: 9178736]
49. Buma P, et al. Cross-linked type I and type II collagenous matrices for the repair of full-thickness articular cartilage defects—A study in rabbits. Biomaterials. 2003; 24(19):3255–3263. [PubMed: 12763453]
50. Veilleux NH, Yannas IV, Spector M. Effect of passage number and collagen type on the proliferative, biosynthetic, and contractile activity of adult canine articular chondrocytes in type I and II collagen-glycosaminoglycan matrices in vitro. Tissue Eng. 2004; 10(1–2):119–127. [PubMed: 15009937]
51. Benya PD, Shaffer JD. Dedifferentiated chondrocytes reexpress the differentiated collagen phenotype when cultured in agarose gels. Cell. 1982; 30(1):215–224. [PubMed: 7127471]
52. Benya PD. Modulation and reexpression of the chondrocyte phenotype; mediation by cell shape and microfilament modification. Pathol Immunopathol Res. 1988; 7(1–2):51–54. [PubMed: 3222207]
53. Chang J, Poole CA. Sequestration of type VI collagen in the pericellular microenvironment of adult chondrocytes cultured in agarose. Osteoarthritis and Cartilage. 1996; 4(4):275–285. [PubMed: 11048624]
54. DiMicco MA, et al. Structure of pericellular matrix around agarose-embedded chondrocytes. Osteoarthritis and Cartilage. 2007; 15(10):1207–1216. [PubMed: 17524677]
55. Emans PJ, et al. Autologous engineering of cartilage. Proceedings of the National Academy of Sciences. 2010; 107(8):3418–3423.
56. Fernandez-Cossio S, et al. Biocompatibility of agarose gel as a dermal filler: Histologic evaluation of subcutaneous implants. Plastic and Reconstructive Surgery. 2007; 120(5):1161–1169. [PubMed: 17898590]

57. Selmi TAS, et al. Autologous chondrocyte implantation in a novel alginate-agarose hydrogel - Outcome at two years. Journal of Bone and Joint Surgery-British Volume. 2008; 90B(5):597–604.
58. Mauck RL, et al. Functional Tissue Engineering of Articular Cartilage Through Dynamic Loading of Chondrocyte-Seeded Agarose Gels. Journal of Biomechanical Engineering. 2000; 122(3):252–260. [PubMed: 10923293]
59. Nakamura A, et al. Osteocalcin Secretion as an Early Marker of In Vitro Osteogenic Differentiation of Rat Mesenchymal Stem Cells. Tissue Engineering Part C-Methods. 2009; 15(2): 169–180. [PubMed: 19191495]
60. Wise JK, et al. Comparison of uncultured marrow mononuclear cells and culture-expanded mesenchymal stem cells in 3D collagen-chitosan microbeads for orthopedic tissue engineering. Tissue Eng Part A. 2014; 20(1–2):210–224. [PubMed: 23879621]
61. Farndale RW, Buttle DJ, Barrett AJ. Improved quantitation and discrimination of sulphated glycosaminoglycans by use of dimethylmethylene blue. Biochim Biophys Acta. 1986; 883(2):173–177. [PubMed: 3091074]
62. Gomoll AH, et al. The subchondral bone in articular cartilage repair: current problems in the surgical management. Knee Surg Sports Traumatol Arthrosc. 2010; 18(4):434–447. [PubMed: 20130833]
63. Lee CR, et al. Effects of harvest and selected cartilage repair procedures on the physical and biochemical properties of articular cartilage in the canine knee. J Orthop Res. 2000; 18(5):790–799. [PubMed: 11117302]
64. Lund AW, et al. Osteogenic differentiation of mesenchymal stem cells in defined protein beads. J Biomed Mater Res B Appl Biomater. 2008; 87(1):213–221. [PubMed: 18431753]
65. Wang L, Rao RR, Stegemann JP. Delivery of mesenchymal stem cells in chitosan/collagen microbeads for orthopedic tissue repair. Cells Tissues Organs. 2013; 197(5):333–343. [PubMed: 23571151]
66. Rao RR, et al. Dual-phase osteogenic and vasculogenic engineered tissue for bone formation. Tissue Eng Part A. 2015; 21(3–4):530–540. [PubMed: 25228401]
67. Peterson AW, et al. Vasculogenesis and angiogenesis in modular collagen-fibrin microtissues. Biomaterials Science. 2014; 2(10):1497–1508. [PubMed: 25177487]
68. Chen Z, Wang L, Stegemann JP. Phase-separated chitosan–fibrin microbeads for cell delivery. Journal of Microencapsulation. 2011; 28(5):344–352. [PubMed: 21736519]
69. Chen HT, Middleman S. Drop size distribution in agitated liquid-liquid systems. AIChE Journal. 1967; 13(5):989–995.
70. Calabrese, RV., et al. Measurement and analysis of drop size in a batch rotor-stator mixer; Proc. 10th Eur. Conf. on Mixing (Delft, Holanda); 2000.
71. McGuigan AP, Sefton MV. Vascularized organoid engineered by modular assembly enables blood perfusion. Proc Natl Acad Sci U S A. 2006; 103(31):11461–11466. [PubMed: 16864785]
72. Tiruvannamalai-Annamalai R, Armant DR, Matthew HW. A glycosaminoglycan based, modular tissue scaffold system for rapid assembly of perfusable, high cell density, engineered tissues. PLoS One. 2014; 9(1):e84287. [PubMed: 24465401]
73. Nichol JW, Khademhosseini A. Modular Tissue Engineering: Engineering Biological Tissues from the Bottom Up. Soft Matter. 2009; 5(7):1312–1319. [PubMed: 20179781]
74. Rao RR, Stegemann JP. Cell-Based Approaches to the Engineering of Vascularized Bone Tissue. Cytotherapy. 2013; 15(11) p. 10.1016/j.jcyt.2013.06.005.
75. Park IS, Rhie J-W, Kim S-H. A novel three-dimensional adipose-derived stem cell cluster for vascular regeneration in ischemic tissue. Cytotherapy. 2014; 16(4):508–522. [PubMed: 24210783]
76. Kittaka M, et al. Clumps of a mesenchymal stromal cell/extracellular matrix complex can be a novel tissue engineering therapy for bone regeneration. Cytotherapy. (0)
77. Lake SP, Hald ES, Barocas VH. Collagen-agarose co-gels as a model for collagen–matrix interaction in soft tissues subjected to indentation. Journal of Biomedical Materials Research Part A. 2011; 99A(4):507–515. [PubMed: 21913316]
78. Lake S, et al. Mechanics of a Fiber Network Within a Non-Fibrillar Matrix: Model and Comparison with Collagen-Agarose Co-gels. Annals of Biomedical Engineering. 2012; 40(10): 2111–2121. [PubMed: 22565816]

79. Tanaka H, Matsumura M, Veliky IA. Diffusion characteristics of substrates in Ca-alginate gel beads. Biotechnology and Bioengineering. 1984; 26(1):53–58. [PubMed: 18551586]

80. Bosnakovski D, et al. Chondrogenic differentiation of bovine bone marrow mesenchymal stem cells (MSCs) in different hydrogels: Influence of collagen type II extracellular matrix on MSC chondrogenesis. Biotechnology and Bioengineering. 2006; 93(6):1152–1163. [PubMed: 16470881]

81. Muhonen V, et al. Recombinant human type II collagen hydrogel provides a xeno-free 3D micro-environment for chondrogenesis of human bone marrow-derived mesenchymal stromal cells. Journal of Tissue Engineering and Regenerative Medicine. 2015 p. n/a-n/a.

82. Wang Y, Sul HS. Pref-1 Regulates Mesenchymal Cell Commitment and Differentiation through Sox9. Cell Metabolism. 2009; 9(3):287–302. [PubMed: 19254573]

83. Warzecha J, et al. Sonic hedgehog protein promotes proliferation and chondrogenic differentiation of bone marrow-derived mesenchymal stem cells in vitro. Journal of Orthopaedic Science. 2006; 11(5):491–496. [PubMed: 17013738]

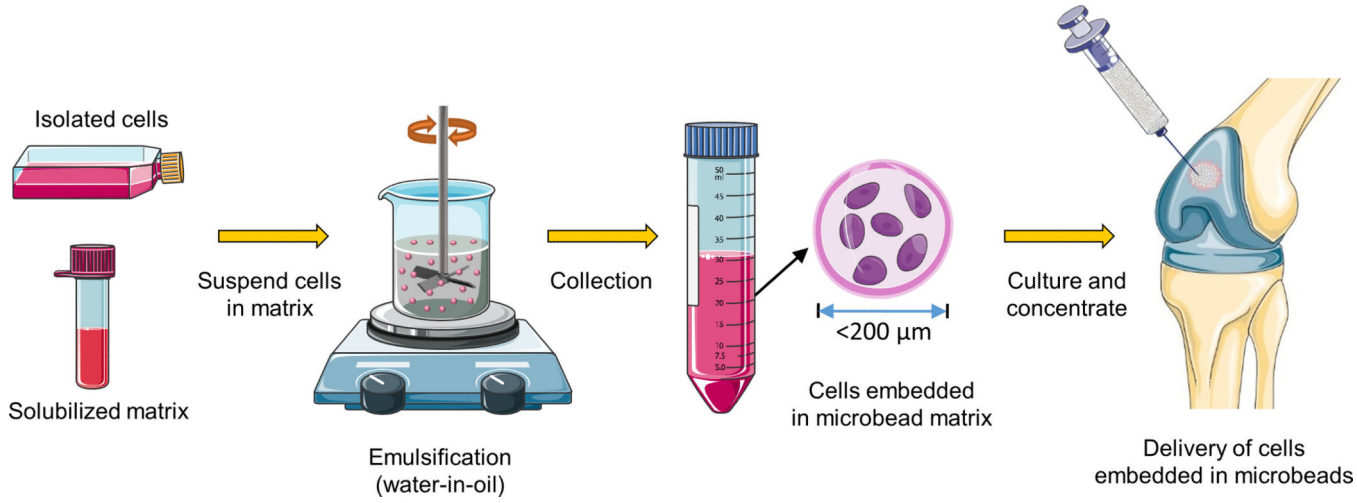

Figure 1.

Schematic of the preparation of injectable microbeads for cartilage repair. A water-in-oil emulsification technique is used to generate spheroidal microbeads containing embedded cells. The microbead matrix consists of agarose and collagen Type II to mimic the composition of cartilage. Microbeads can be cultured in suspension and delivered via injection, and their small size facilitates mass transport to the embedded cells. The long-term goal is to develop an injectable, living articular cartilage tissue analog. Parts of this figure were obtained from Servier Medical Art (www.servier.com).

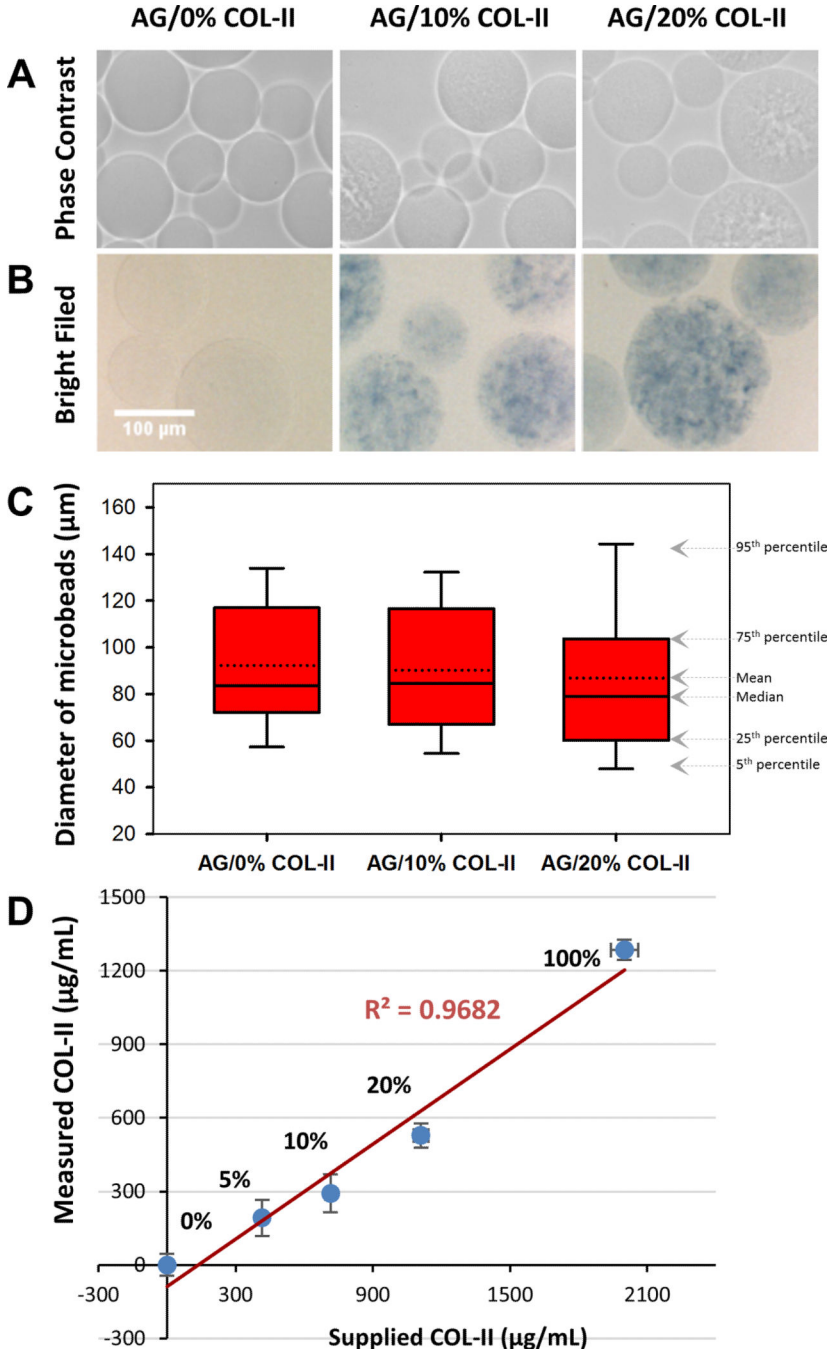

Figure 2.

Morphology, collagen content, and size distribution of AG/COL-II microbeads. (A) Phase contrast and (B) brightfield images of acellular microbeads with varying COL-II concentration, with collagen stained with Coomassie Blue in the brightfield images. (C) Diameter of microbeads as a function of composition. The solid center line in the box plot represents the median, the dotted center line in the box represents the mean, and the lower and upper boundaries of the box represent the 25th and 75th percentiles, respectively.

Whiskers (error bars) above and below the box indicate the 90th and 10th percentiles. (D) Quantitation of protein content of AG/COL-II microbeads using a total protein assay.

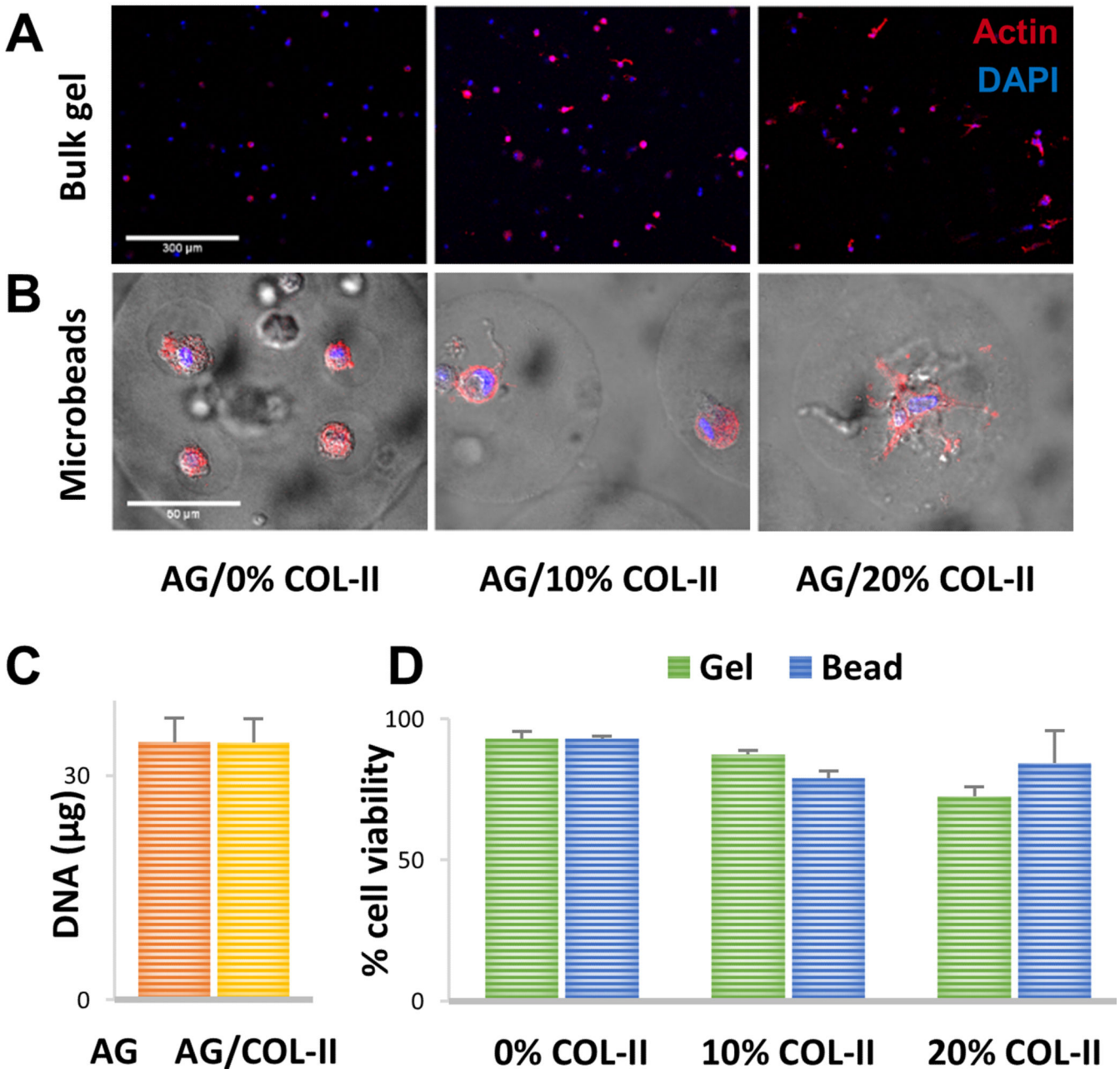

Figure 3.

Cell morphology and viability in bulk gels and microbeads. (A) Fluorescence staining of actin cytoskeleton (red) and nucleus (blue) of MSC embedded in bulk gels. (B) Fluorescence staining of actin cytoskeleton (red) and nucleus (blue) of MSC embedded in AG/COL-II microbeads with overlay of brightfield image to visualize microbead boundaries. (C) DNA content of microbeads made with pure AG or AG/10% COL-II one day after microbead fabrication. (D) Percentage of viable cells in bulk gels and microbeads one day after gel fabrication. Images best viewed in color.

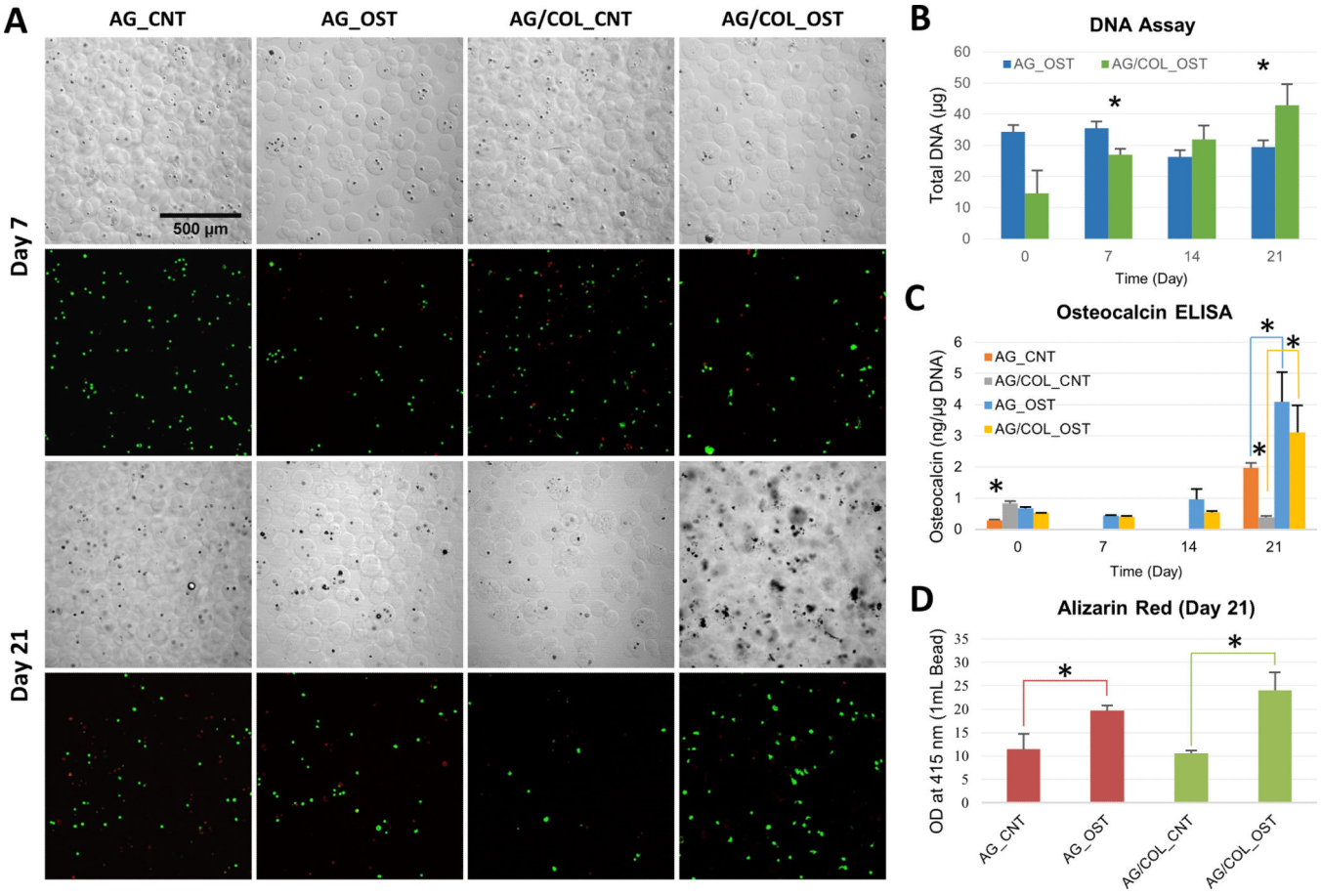

Figure 4.

Osteogenic differentiation of MSC in microbeads. (A) DIC images of microbeads with corresponding Live/Dead® confocal fluorescence images at day 7 (top two rows) and day 21 (bottom two rows). (B) DNA content of AG and AG/COL-II microbeads over time in culture. (C) Osteocalin production by hMSC in AG and AG/COL-II microbeads over time in culture. (D) Calcium phosphate mineral deposition by hMSC in AG and AG/COL-II microbeads over time in culture. All images at same magnification. (*) indicates $p<0.05$. Best viewed in color.

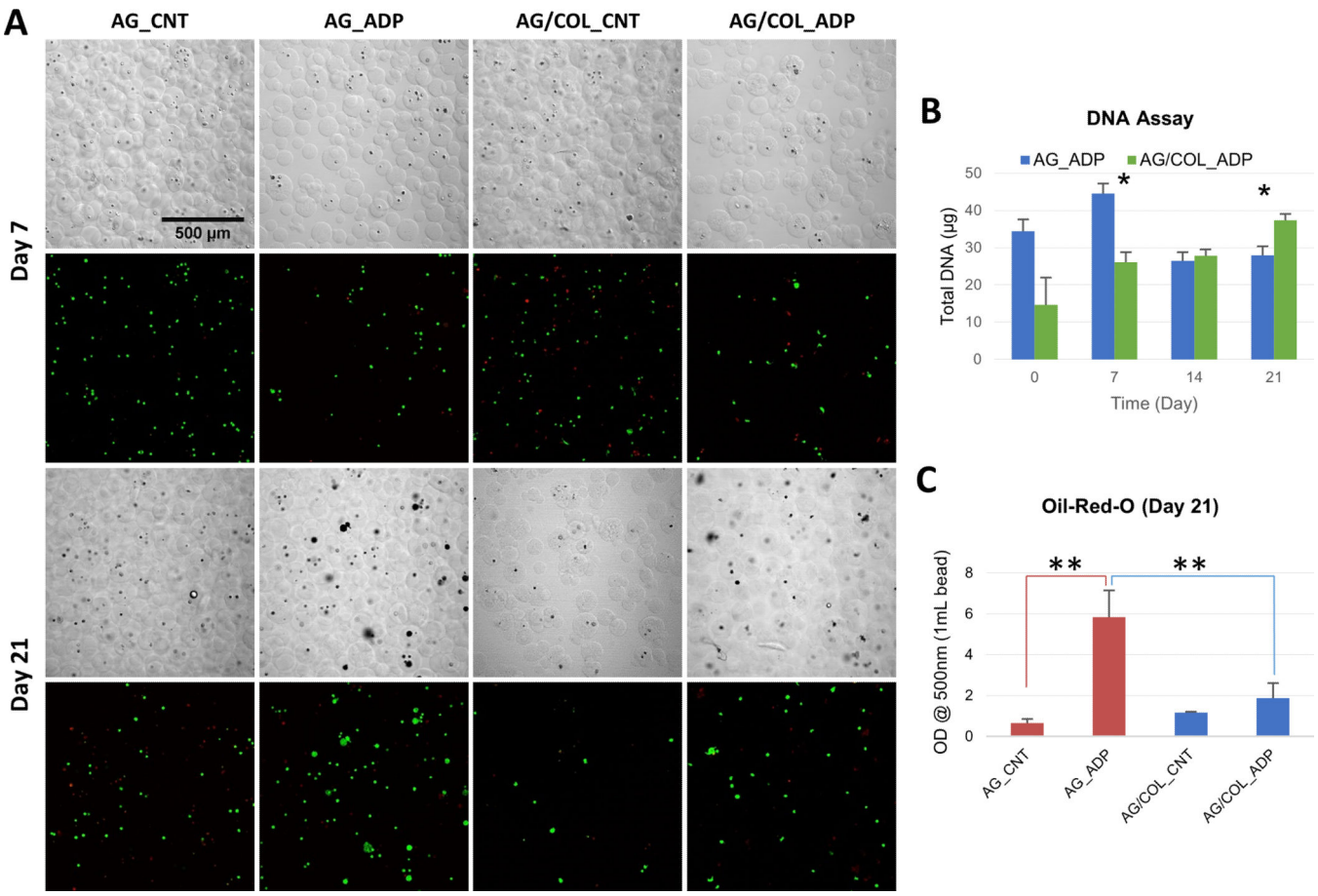

Figure 5.

Adipogenic differentiation of MSC in microbeads. (A) DIC images of microbeads with corresponding Live/Dead® confocal fluorescence images at day 7 (top two rows) and day 21 (bottom two rows). (B) DNA content of AG and AG/COL-II microbeads over time in culture. (C) Intracellular lipid droplet accumulation in AG and AG/COL-II microbeads over time in culture. All images at same magnification. (*) indicates $p<0.05$. (**) indicates $p<0.001$ Best viewed in color.

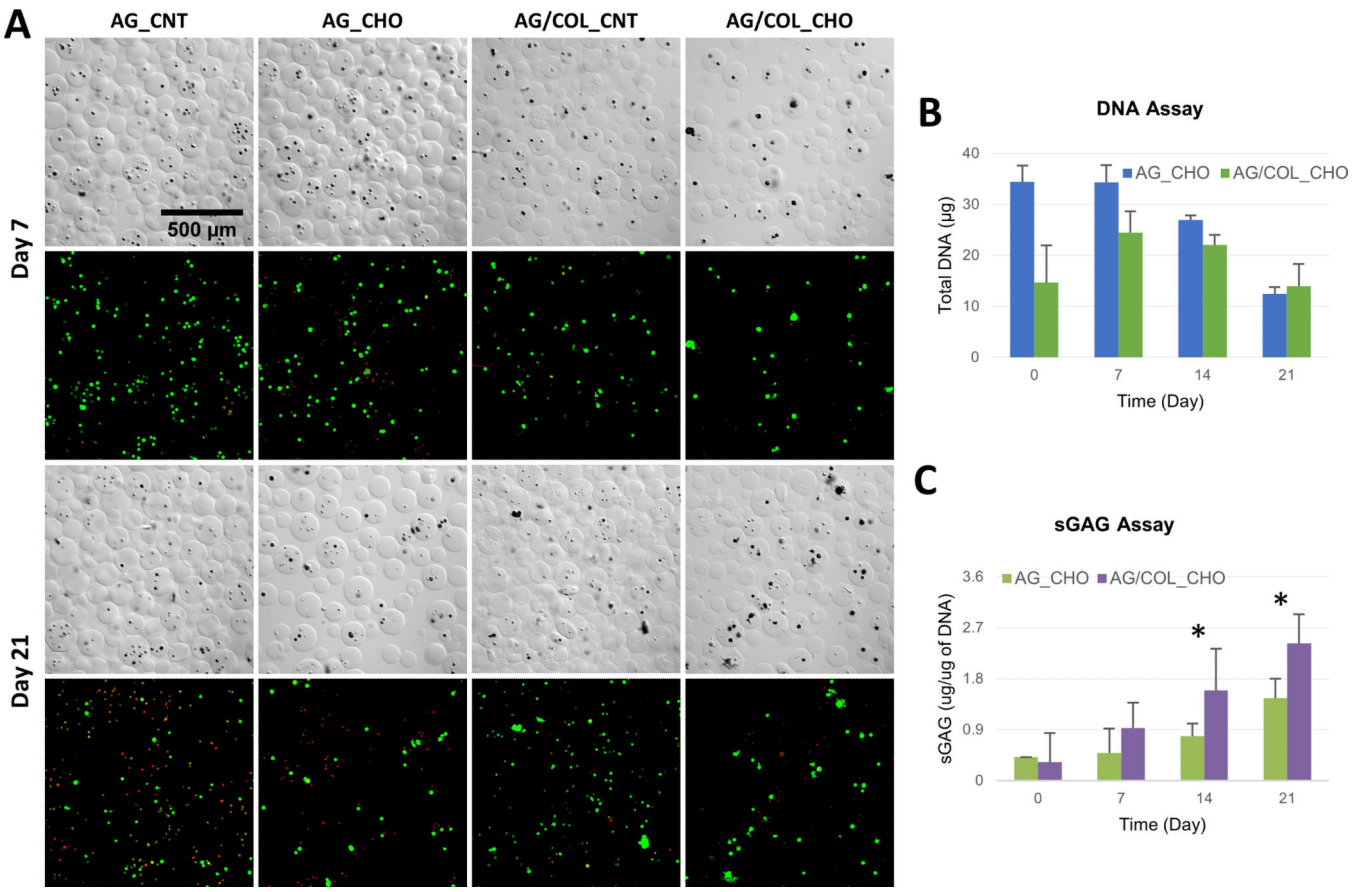

Figure 6.

Chondrogenic differentiation of MSC in microbeads. (A) DIC images of microbeads with corresponding Live/Dead® confocal fluorescence images at day 7 (top two rows) and day 21 (bottom two rows). (B) DNA content of AG and AG/COL-II microbeads over time in culture. (C) Sulfated glycosaminoglycan (sGAG) production by MSC embedded in AG and AG/COL-II microbeads over time in culture. All images at same magnification. (*) indicates $p<0.05$. Best viewed in color.

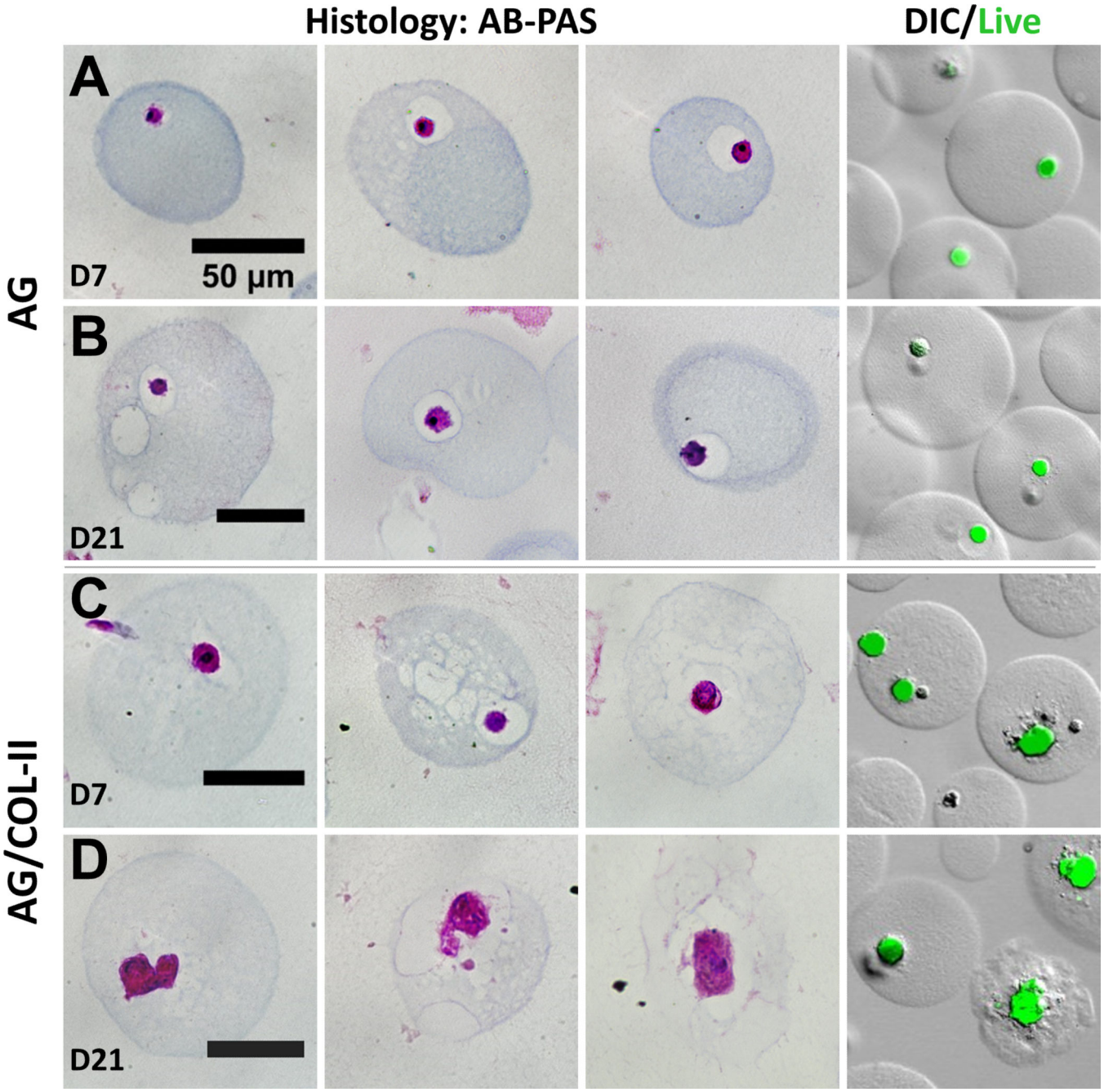

Figure 7.

Histological evaluation of microbeads in chondrogenic medium at day 7 and day 21. First three columns show representative microbeads stained with Alcian Blue (AB)-Periodic Acid Schiff (PAS), and fourth column shows cells in microbeads stained with calcein-AM with overlay of DIC image of microbeads. (A, B) pure AG beads. (C, D) AG/10% COL-II beads. Best viewed in color.

Table 1

Volumes of AG, COL-II, NaOH and FBS used to create collagen-agarose bead formulations.

FORMULATIONS	AG* (μL)	COL-II** (μL)	NaOH (μL)	FBS (μL)	α-MEM (μL)
*AG/**0%** COL-II*	1500	0	0	300	1200
*AG/**10%** COL-II*	964	536	107	300	1093
*AG/**20%** COL-II*	667	833	167	300	1033
*AG/**100%** COL-II*	0	1500	300	300	900

% COL-II is given as wt/wt (collagen/agarose).

* AG stock concentration is 20 mg/mL of DI water (2 wt%);

** COL-II stock conc. is 40 mg/mL of 0.02 N acetic acid (0.4 wt%).

Table 2

Quantification of cell viability in AG and AG/COL-II microbead formulations

Time	Culture Media	Total no. of cells	% Live cells	% Dead Cells	Total no. of cells	% Live cells	% Dead Cells
	n=3		**Agarose**			**Agarose/Collagen-II**	
Day 7	Expansion	357	92	8	348	61	39
	Osteogenic	210	60	40	204	72	28
	Adipogenic	171	77	23	111	62	38
	Chondrogenic	159	60	40	174	67	33
Day 21	Expansion	245	50	50	48	69	31
	Osteogenic	174	67	33	270	88	12
	Adipogenic	306	63	37	165	80	20
	Chondrogenic	453	32	68	147	59	41